High-pressure phases of the alkali metals

N. E. Christensen
Institute of Physics and Astronomy, Aarhus University,
DK-8000 Aarhus C, Denmark
D. L. Novikov
Arthur D. Little Inc., Acorn Park,
Cambridge, MA 02140-2390, USA

Abstract

A series of recent x-ray diffraction experiments carried out by scientists from the Max-Planck-Institut FKF in Stuttgart and the ESRF in Grenoble on elemental semiconductors and alkali metals under high pressure have provided new insight in pressure induced structural transformations. New structures have been identified, and some of these have surprising similarities, such as low coordination numbers. The new lithium phase, Li-cI16, which has a cubic structure with 16 atoms in the cubic cell, has not been found for any other element. Theoretical studies, some of which are described here, using *ab initio* methods to calculate electronic and structural properties provide theoretical support for the analysis of these experiments, and may also serve to predict new properties, such as superconductivity, of the materials when exposed to very high pressures.

Introduction

The alkali metals, earlier considered as *simple metals* with bandstructures that differ only slightly from those of free-electron systems, have attracted considerable [1] interest because application of external pressure changes the bonding properties fundamentally. For example lithium, the first monovalent metal in the Periodic Table, is sometimes expected to be a model system of hydrogen, where the atoms form diatomic molecules in insulating solid phases. The breaking of the bonds in hydrogen by applying very high pressures is a *Holy Grail* of physics[1], and it is important for the understanding of the metallic hydrogen in the interior of the heavy planets. In view of this it was remarkable that theoretical calculations by Neaton and Ashcroft[2] predicted that compressed Li might assume a structure (*oC8* with i*Cmca*

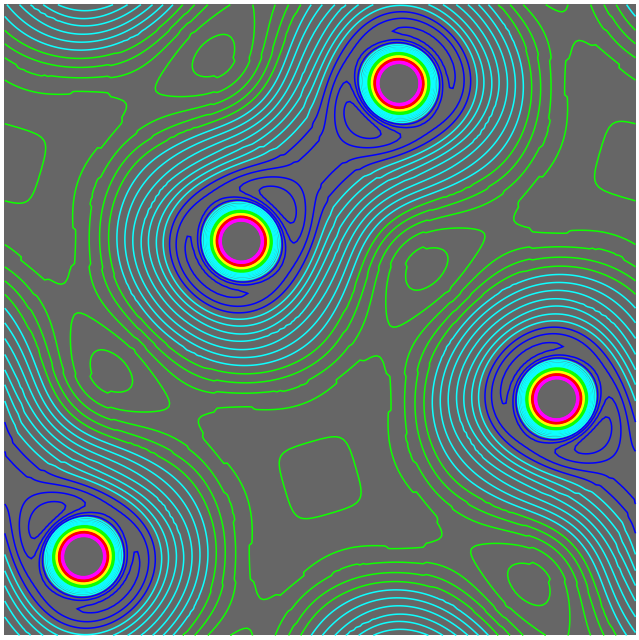

Figure 1: Contour plot of the calculated valence-electron density in lithium in the BC8 structure at 165 GPa (V/V_0=0.23). The colour coding is dark blue towards red/magenta for increasing density. The lowest contour value is 0.0472 $Å^{-3}$, the increment is 0.0135 $Å^{-3}$. Disregarding the innermost core oscillations, the highest valence density is found in the interstitial square-like green contour, $1.4\times\rho_{av}$, where ρ_{av}=0.204 $Å^{-3}$ is the average density.

symmetry) where the atoms form *pairs*, and that this phase is semi-insulating. This is in sharp contrast to the intuitive expectation that application of hydrostatic pressure should favour highly coordinated metallic phases.

The compressibilty of the alkali metals is very large, and the large volume reduction with application of pressure affects significantly the otherwise free-electron like electronic structure. As a consequence, these metals undergo several pressure-induced structural transformations. These have been studied experimentally (see for example Ref. [3, 4, 5, 6, 7, 8, 9]) as well as by theoretical methods (Ref. [2, 3, 9, 10, 11, 12, 13, 14] and references therein). Among several interesting results of this research, the most recent progress includes the observation[3] of new high-pressure phases of lithium, Li-*hR1* and Li-*cI16*, and the identification[6, 15] of the structure of Cs-V and Rb-VI as being the orthorhombic *Cmca* structure with 16 atoms in the orthorhombic unit cell (*oC16*). The same structure type, with very nearly the same relative atomic coordinates, is found in Si and Ge under pressure.[7, 12, 16, 17, 18] This *Cmca* structure contains two types of atoms, say Cs_1 and Cs_2, with Cs_1 in planar arrangements separating Cs_2 double layers. The atoms in the single planes form a dense packing of *dimers*.[12] This has some similarity with the Cmca structure predicted for Li under pressure by Neaton and Ashcroft.[2] In that structure (*oC8*), however, the double layers of type-2 atoms are absent, i.e. the structure is similar to that of Ga at ambient pressure.

In Fig. 1 we show, as an example of such a ”paired structure”, the distribution of valence electrons in lithium at 165 GPa. The apparent formation of atom *pairs*, however, should not be overemphasized. It is true that there is a single, shortest interatomic distance, but the next-nearest neighbours in the Cmca structures are not much further away. Therefore the ”effective” coordination number is rather $\approx$5 than

one. The interesting result, though, is that there is a tendency of formation of low-coordinated phases of highly compressed alkali metals. Further, as the results of the calculations will show, the bonding is very different from usual molecular (covalent) bonding. Already, the density plot, Fig. 1, demonstrates this.

The pressure-driven electronic $s \rightarrow d$ transition [19] plays a major role in the structural behavior of cesium,[11, 20] in particular the ocurrence of the tetragonal CsIV phase which is only eightfold coordinated.[5] The unusual decrease of the coordination number with increasing pressure from 12 in *fcc* to 8 in CsIV has been interpreted in terms of a peculiar directional bonding induced by the *s-d* transition.[20, 21] This leads to a softening and a dynamical instability in Cs-II (fcc).[13, 14] Also, the thermal expansion coefficients of Cs have been predicted to be negative at all temperatures in certain pressure ranges.[13, 14] The light alkali metals, Li and Na, are similarly strongly influenced by an $s \rightarrow p$ transition.

Structures and Method of Calculation

The *ab initio* simulation methods which we apply cannot be used to perform an ideal, molecular dynamical structural optimization. We must select a certain set of structure types, i.e. space groups and number of atoms in the cells. Some of the structures, however, will have parameters, like axial ratios and atomic site parameters, which must be optimized at each volume (pressure). We can then, among the structures included in the set, determine which one is stable, statically as well as dynamically, at a given volume. In that way one can never be sure to find the 'true' ground state structure, but the procedure will be given relevance in describing trends and binding properties to be expected if the structures to be examined are selected in a 'sensible manner'.

The simplest close-packed structures, *bcc, fcc, hcp dhcp*, body-centered cubic, face centered cubic, and hexagonal close packed are well-known. The *hcp* stacking sequence in the c-direction is ABA. Similarly, *fcc* and *bcc* can be built by stacking (111)-layers in the sequence ABCA. In this hexagonal representation, *fcc* has $c/a = \sqrt{6}$, and for *bcc* the axial ratio is $c/a = \frac{1}{2}\sqrt{3/2}$. The so-called ω-phase structure appears if the B and C layers i *bcc* are shifted so that they coalesce at $z = c/2$. The double-hexagonal close-packed structure (*dhcp*) has an ideal c/a ratio which is twice that of hcp, and the stacking is ABACA. The "samarium type structure", *9R*, is a nine-layer hexagonal structure, stacking ABABCBCACA. Calculations are most conveniently performed using the primitive rhombohedral cell which contains only 3 atoms. Also *A7* (space group 166 in the International Tables) has a rhombohedral primitive cell. It contains two atoms. For special parameters, *A7* becomes the simple cubic, *sc*, structure. The simple rhombohedral structure, *hR1*, is obtained by straining the *fcc* structure along a body diagonal. The structure which is called *cI16* belongs to the spacegroup $I\bar{4}3d$ (number 220 in the International Tables). This was found experimentally for Li under pressure[3], and sofar it has not been observed for any other elemental solid. The atoms are located in the *16c* Wyckoff positions. The primitive cell is *bcc*. The *oC8* structure is of Cmca symmetry, and it resembles that of α-gallium, but can also ve viewed as that of black phosphorous compressed perpendicularly to its double layers.

Some of the high-pressure phases have structures similar to the cation sublattices of binaries,[3] and the structure of CsIV[5] is an example of this. CsIV forms in a tetragonal structure with $I4_1/amd$ symmetry, SG 141, and the atoms are placed in

$$\mathbf{r}_1 = (0,0,0); \mathbf{r}_2 = (0, \frac{1}{2}, \frac{c}{2a}). \quad (1)$$

This is the structure of the Th sublattice in $ThSi_2$.[22] The *cI16* structure described above is in fact that of the the cation sublattice in Eu_4As_3 and Yb_4As_3, i.e. anti-Th_3P_4 structures.[23] As mentioned *cI16* is a cubic structure with a bcc Bravais lattice and 8 atoms in the rhombohedral primitive cell. Several other cubic structures may be generated by distorting such a bcc supercell. As one example we consider the *BC8* structure, mainly because it has been found, as also *R8*, in metastable Si phases. The *BC8* structure[24] is also body-centered-cubic with 16 atoms in the unit cell (8 atoms in the primitive cell). The space group it $Ia\bar{3}$, and the atoms are in the 16*c* Wyckoff sites, (x_0,x_0,x_0). It may also be viewed as a rhombohedral structure with an 8-atom primitive cell, SG $R\bar{3}$. This has 2 atoms in the 2*c*, (u,u,u) and 6 in the 6*f*, (x,y,z), sites. These parameters are related to x_0 by u=2x_0, x=1/2, y=0, and z=1/2-2x_0. Thus, in *BC8* there is one internal parameter (x_0) which must be optimized.

The *BC8* structure can be considered as a special setting of the structural parameters of the *R8* structure. Both have the SG $R\bar{3}$ (number 148). The 8 atoms in the R8 primitive cell are located are the 2c, (u,u,u), and the 6f, (x,y,z), Wyckoff sites. In *BC8* all 8 sites are equivalent, but in *R8* the 2c and the 6f sites are inequivalent. The Si-*BC8* and -*R8* phases are described in Ref. [25].

The total energy for a given choice of atomic coordinates is calculated within approximations to the density functional theory, the local approximation (LDA) as well as a generalized gradient approach (GGA). The results presented here are obtained with the GGA, and we used the Perdew-Burke-Ernzerhof scheme.[26] The solution of the effective one-electron equations is performed by means of the linear muffin-tin-orbital (LMTO) method [27] in the full-potential version. [28] The semi-core states, Li-1*s*, Na-2*s*, and Na-2*p*, are treated as *local orbitals*[29] in the same energy window as the valence states. The bandstructure calculations are scalar relativistic, i.e. all relativistic effects, except spin-orbit splittings, are included.

The structural optimization required in all cases except for the *bcc* and *fcc* structures is made at each of 21 volumes, V, in the range $0.10\times V_0$ to $1.10\times V_0$, where V_0 is the (experimental) equilibrium volume of bcc-Na at ambient pressure. (We use V_0=21.2725 Å^3 for Li and 37.7073 Å^3 for Na). For some structures, like *hcp*, *dhcp*, and *hR1*, only a single, internal parameter needs to be varied, but other cases require more time consuming optimizations. A7 and 9R require optimization of two parameters, z and c/a. In the Cmca structures we need to vary the axial ratios, c/a and b/a, as well as 2 (in *oC8*) or 3 (in *oC16*) internal parameters. Also for *R8* there are 5 parameters to be optimized simultaneously. This is done by means of a steepest-descent method.

Results

Having calculated the optimized total energies, E, vs. volume for all structures, and applying a least-squares fit to a power series in $X = (V/V_0)^{1/3}$ (positive as well as negative powers), we derive pressure, P, bulk modulus, B, and enthalpy, $H = E + PV$. The calculated $P-V$ relations are then used to calculate $H(P)$, and the results are summarized in Fig.2. The calculated pressures for some of the compressed Na phases are shown in Fig. 3.

The *dhcp* structure is not included since it is close in energy to *hcp*. Also, the calculations for *oC16*

have been omitted, since for Na (as for Li) it is above the other structures in energy. At low pressures (not visible on the scale of Fig.2) we find that the *bcc* structure is favoured in sodium. The calculation predicts that this remains the stable structure up to $P_{t1} \approx 80$ GPa, where it transforms to the *fcc*. It should be noted, however, that the the maximum difference, $E(fcc) - E(bcc)$ is only 5 meV/atom. (We find the same differences using LDA). The fact that we find the energy difference to that small also implies that a substantial error bar is associated with the value of P_{t1}, and we there also made independent calculations using the FP-LAPW method as implemented in the WIEN97 code.[30] Very similar results were obtained.

The instability of Na-*bcc* is also reflected in the volume dependence of the elastic shear constants. As found by Katsnelson et al.[10] and also in the calculations[13, 14] for Cs, $C^{'}$ and C_{44} soften and tend to go negative under compression. Another distortion of the *bcc* structure of sodium could be possible, namely that to the ω-phase.[31] At high pressures, Fig.2 clearly shows that Na-ω cannot be a stable structure.

The (perfect) *fcc* (red-orange in Fig.2) structure remains stable up to ≈170 GPa, where it becomes unstable against a rhombohedral shear. The elastic constant C_{44} goes negative, and the fcc-lattice bcomes dynamically unstable. This signals the transition to the distorted structure, *hR1* (orange). The *cI16* structure starts to be the favoured structure at $P_{t2} \approx$170 GPa. The figure shows how a hypothetical *bcc* becomes unstable towards *x*-distortions around 130 GPa, and at P_{t2} the energy gain associated with these displacements has become so large that *cI16* enthalpy value is the same as that of *hR1*. However, in the very same pressure regime Na-*CsIV* rapidly lowers its free energy with pressure so much that it becomes the lowest among those examined up to $P_{t3} \approx 220$ GPa, where the *Cmca* structure, *oC8* takes over. The figure shows that with the error bars the onset of Na-*cI16* may be somewhere between 110 and 170 GPa if observed at all. The displacements, *x*, increase with compression, as in Li,[3], but in Na *x* seems to approach a limiting value of 0.065 at extreme compressions. This is different from Li, where a saturation value of 0.125 was found.[3]

Apart from the range around 170 GPa where several structures are close in energy, the hexagonal structures, *hcp* and *dhcp*, are not likely to be "good candidates" for Na at high pressure, and it is so although although substantial energy can be obtained by reducing c/a at small volumes.

The three *coexistence pressures* P_{t1}, P_{t2}, and P_{t3} are also marked in Fig.3 which shows the calculated $P-V$ relations for some selected structures of Na at small volumes. From low pressures (in fact from 0) up to 120 GPa we find that the pressures of the close-packed phases follow each other closely. The change of slope in $P(V)$ for *hcp*-Na structure around 270 GPa reflects a rapid change in c/a upon compression.

For Li it was demonstrated that a the distortion (finite *x* value in Fig. 2 of Ref. [3]) of the *bcc* structure into *cI16* causes the formation of a pseudo-gap, and thus to a downshift in an appreciable amount of filled electron states. The one-electron energy sum is similarly reduced in Na-*cI16* as *x* becomes non-zero. A similar effect is found in the *CsIV* and the *BC8* structures. Again the formation of a pseudogap near E_F tends to stabilize the structure. In all cases the increasing occupation of *p* states with pressure is essential for the formation of the new structures, and this is most spectacular in Na-*oC8*, the phase which is clearly the lowest in energy among those examined in the high-end of the pressure range of Fig. 2. The pseudogap which is present even at V/V_0=0.45 becomes rapidly deeper as the lattice is compressed, and at the smallest volume examined for Na, V/V_0=0.10, its DOS at E_F vanishes, Fig. 4. In fact a very small, finite gap has formed. In Li-*oC8* it was also found[2, 3] that DOS(E_F) vanishes at a very high pressure, but the energy-optimized structure did not exhibit a finite gap. The $s \rightarrow p$ transition responsible for this

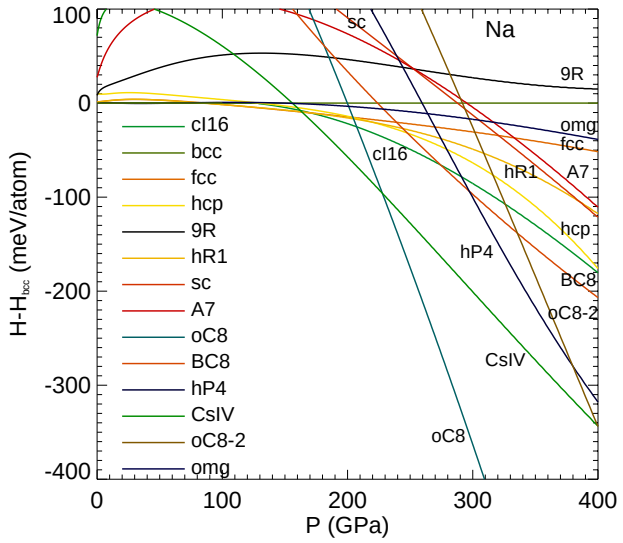

Figure 2: Enthalpies of 10 Na phases vs. pressure (P). The enthalpy of the bcc structure is used as a reference.

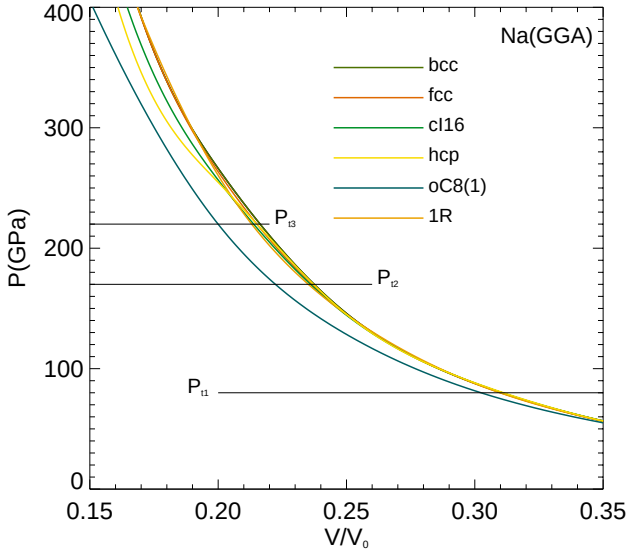

Figure 3: Calculated pressures vs. volume for Na in selected structures (only the range between 0.15 and 0.35 V_0 is shown). The pressures P_{t1}, P_{t2}, and P_{t3} are the calculated pressures of transition from *bcc* to *fcc/hR1*, *hR1* to "CsIV", and "CsIV" to Na-*oC8*, respectively.

behavior is further illustrated in Fig. 5.

A similar strong increase in the ratio between *p*- and *s* electron counts at large compressions was found for Li. At first, such a behavior might be explained for Li as an effect of orthogonality; the Li atom has a full *s* core, and the 2*s* valence states are kept away from the core regime, even at small volumes due to their orthogonality to the 1*s* states. Orthogonality does not impose a similar *radial* constraint on the Li-2*p* states, and consequently the 2*p* *canonical* band[27] can increase its overlap with the Li-2*s* band when Li is compressed.

A similar argument cannot be applied to Na. In that case the core of the atom contains *s*- as well as

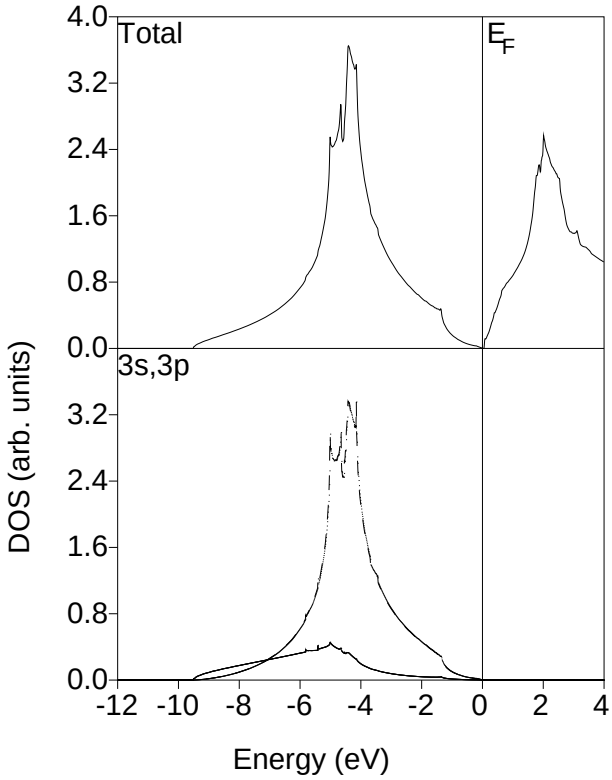

Figure 4: Density-of-states functions for Na in the *oC8* structure at V/V_0=0.10.

p-states ($2p$), and a weaker $s \rightarrow p$ transition should then be expected. But the behaviour in sodium is as that of lithium.

Hybridization is very strong in the compressed alkali metals. If we consider a hypothetical Na-*fcc* crystal at the smallest volume, V=0.1V_0, considered here, its interatomic distance is 1.73 Å. This is the same as the distance from the nucleus of the free Na atom to the outer maximum of the Na-3*s* wavefunction.[32] Consequently, a 3*s* wavefuntion from a nearest neighbour atom in the compressed solid will, when expanded in around the local site, yield a very large *p* component. Only *s* states have non-vanishing amplitudes on the nucleus, and therefore the crystal structure adjusts so that there are interstitial regimes where the valence charge can pile up. This means that the coordination number is reduced to a lower value than in *fcc*, for example.

The valence electron distribution calculated for Na-*oC8*, see Fig. 6 is very similar to that found in the Li calculations. ”Pairs” of atoms can be seen, but, as mentioned earlier, the next-nearest neighbour distances are close to the shortest interatomic distance, and it is not very meaningful to characterize this as a solid with coordination number 1. The density plot, Fig. 6, further shows that the structure has some similarity with *hP4*, that of graphite, and this is even more so in *oC8-2*, the Cmca structure derived from the Si sublattice in $MoSi_2$.

We have already at several places compared the Na results to experimental and theoretical results presented recently for lithium.[3, 2] Nevertheless, it is worthwhile to compare to a larger set of data than the one which was included in our calculations in Ref. [3]. Figure 7 summarizes enthalpy calculations for 14 out 16 examined structures.

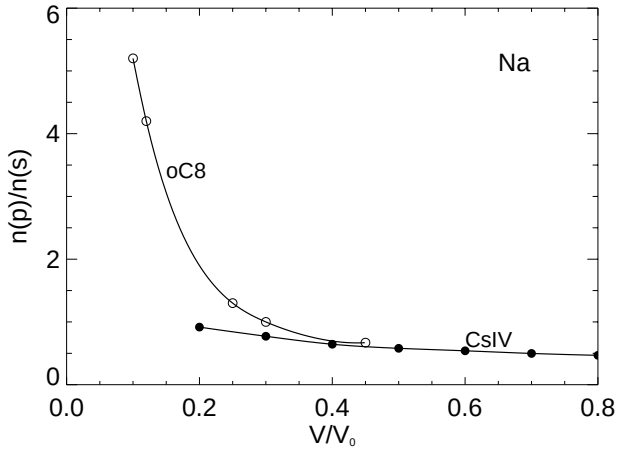

Figure 5: Ratios between the number of *p*- and *s*- valence electrons in two Na-phases vs volume.

Those not included are *oC16* (”CsV”) and *R8*. The former has energies which are well above the reference in Fig. 7, and Li-*R8* was found to converge to Li-*bcc* at low pressures and to Li-*BC8* at high pressures. Among the new results which are interesting, we mention those of Li-*hP4* (graphite type) and Li-*CsIV*. Li-*hP4* becomes a competitor to Li-*oC8* at very high pressures, and the calculations show that it has the lowest enthalpy above $\approx$ 300 GPa. The *CsIV* structure i even more interesting since its energy becomes very close to that of Li-*cI16* in a pressure range which may be accesssed experimentally. The upper pressure attained in the measurements of Hanfland and Syassen[3] is around 55 GPa, and the present calculations suggest that there could be a pressure window starting a bit higher where Li-*CsIV* might be found. The smallest energy difference between Li-*CsIV* and -*cI16* in the calculation is 1-2 meV/atom, i.e. well below our error bars.

Comparing Fig. 1 to Fig. 8 we see that at high pressure the valence electrons in Na distributed similarly to those of Li. The shapes of the contours between the atoms in the ”pair” resemble those of covalent bonds. But the nature of the bonding is far from being a conventional diatomic molecular bonding. The blue contours indicate *minimal* densities. The valence electrons are in the interstitial regimes, and the bonding may be considered as a multicenter bonding. The bonding in the high-pressure phases of Li and Na, for example in the *oC8*, is thus quite different from from that in the SiVI phase (*oC16*, also Cmca), see for example Fig. 6 in Ref. [33]. In view of this, it surprising how similar some of the high-pressure phases of the alkali metals are in structure to some of those found in Si and Ge. Apart from having different relative coordinates (x_0 is different) the *BC8* structure of silicon resembles that of Li-*BC8*, but the bonding is quite different. Figure 9 shows our calculated density in Si-*BC8*. This may crudely be described as an ”inverse” of the Li- and Na plots.

Conclusions

Sodium and lithium both assume several, rather complex structures under pressure. Examination of the band structures and orbital-projected density-of-states (DOS) functions show that the number of *p*-states is found to increase at the expense of *s* states under compression. The reason is that the interatomic distances become small compared to the range of the wavefunctions, and the high-pressure phases be-

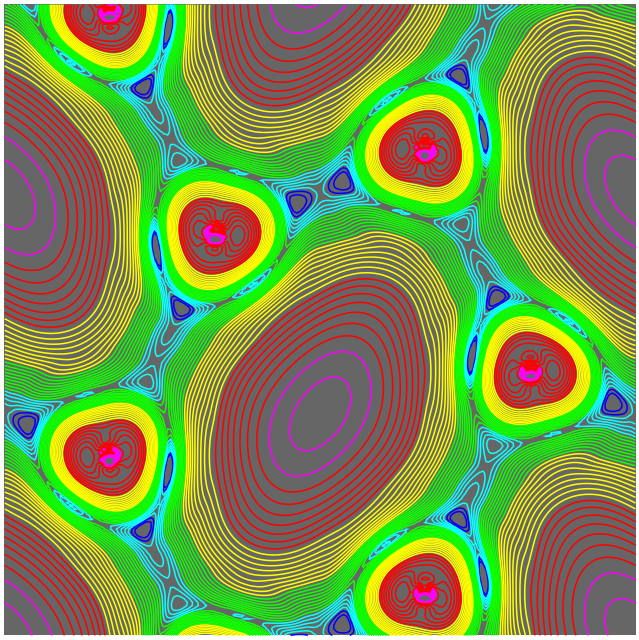

Figure 6: Density of valence electrons in Na-*oC8* at V/V_0. Note that the lowest densities are shown in blue, whereas the red (magenta) correspond to high (highest) densities.

come rather open. Therefore, the structures found theoretically to be good candidates for sodium under very high pressures are characterized by having coordination numbers which are lower than those of the intermediate-pressure phases, *bcc* and *fcc*.

The structural energy differences calculated here do not include thermal effects, i.e. vibrational contributions to enrgy and entropy[13, 14] are neglected. This adds to the error bars of some of the tiny free energy differences. Within such limitations, the calculations cannot clearly distinguish between the *fcc*, *bcc* and the *R9* structures at zero pressure. At slightly elevated pressures, though, *bcc* is favoured, and a *bcc*$\rightarrow$*fcc* transition is predicted near 80 GPa. The error bar is large, probably $\pm$ 20 GPa. Na-*fcc* undergoes a rhombohedral deformation, and close to 180 GPa several new structures become energetically possible. Among these the *cI16* is an interesting candidate, because this structure was experimentally observed[3] for Li under pressure. But also in this case the error bars, at best 5 meV/atom, on the energy difference calculations combined with the slow variation of enthalpy with P implies that a theoretical estimate of the stability range of Na-it cI16 is difficult to give. If observed at all, the lower limit on the onset pressure would be around 110 GPa, and upper limit of its pressure range would be near 170 GPa. Among the structures examined here we find that Na-*CsIV* is lowest in enthalpy between 170 and 220 GPa. Above $P \approx 220$ GPa we find that the Na-*oC8*, Cmca, may be stable up to very high pressures. The structure of Na-*oC8* is similar to the Li-*oC8* phase, but the structural parameters, y, z, b/a, and c/a (not shown here) vary somewhat differently with volume.

Highly compressed Na contains even more 3p- than 3s states, and in the *oC8* the hybridization is so strong that the hybrization gap makes the DOS vanish at the Fermi level in the most compressed cases. (In that context, see also the discussion by Neaton and Ashcroft[2] of the Peirls distortion in Li). The metal-insulator transition occurs in Na only at extreme compression. At 88 % compresssion the *Cmca* phase is still metallic, but reduction of the volume to $0.10\times V_0$ produces a tiny gap according to the calculations. The corresponding pressure is $\approx$ 950 GPa, roughly 3 times the pressure at the center of the

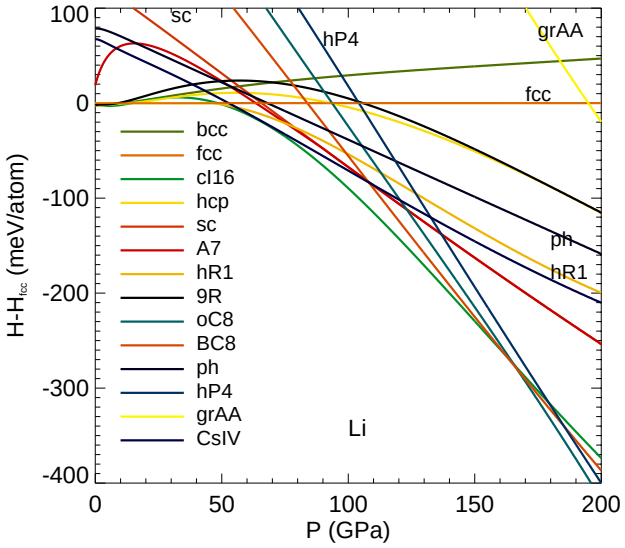

Figure 7: Calculated enthalpies for various Li phases vs. pressure relative to Li-*fcc*. (Note that the *bcc* was used as a reference in the case of Na).

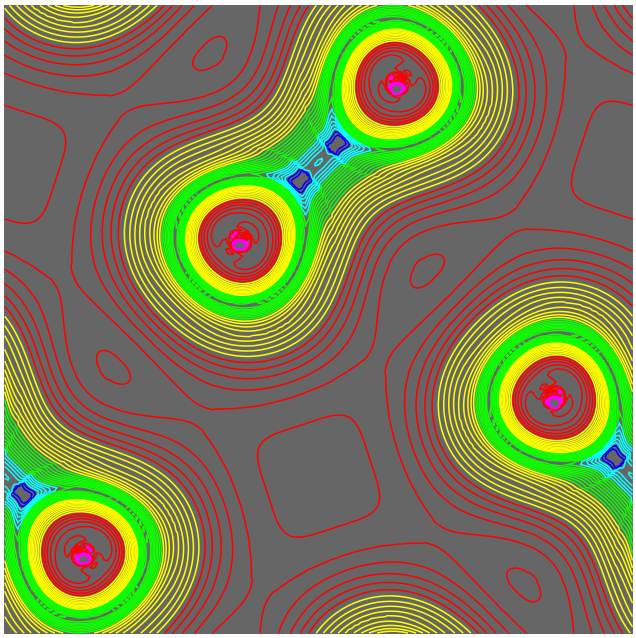

Figure 8: Contour plot of the calculated valence-electron density in sodium in the BC8 structure. Blue contours correspond to the lowest desities, red and magenta to the highest.

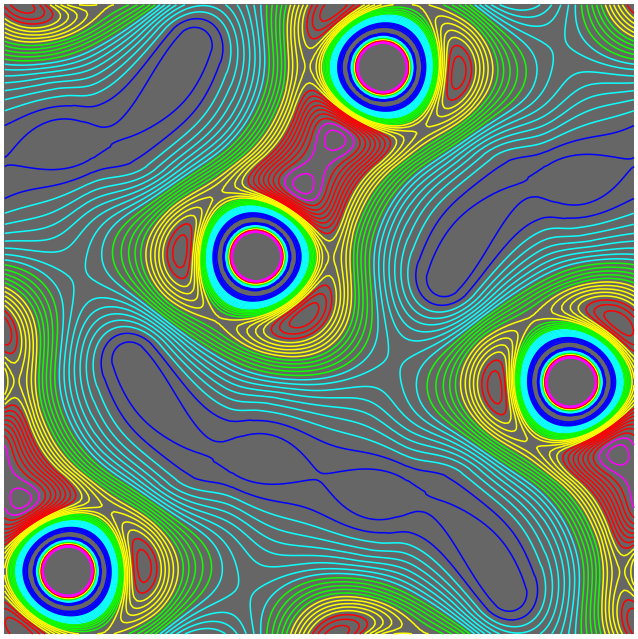

Figure 9: Contour plot of the calculated valence-electron density in silicon in the BC8 structure. Blue contours correspond to the lowest desities, red and magenta to the highest.

Earth. For comparison, *bcc*-Na would need $\approx$ 1500 GPa to be compressed to V/V_0=0.10.

References

[1] R.M. Martin, Nature **400**, 117 (1999).

[2] J.B. Neaton and N.W. Ashcroft, Nature **400**, 141 (1999).

[3] M. Hanfland, K. Syassen, N.E. Christensen, and D.L. Novikov, Nature **408**, 174 (2000).

[4] H. T. Hall, L. Merrill, and J. D. Barnett, Science **146**, 1297 (1964).

[5] K. Takemura, S. Minomura, and O. Shimomura, Phys. Rev. Lett. **49**, 1772 (1982).

[6] U. Schwarz, K. Takemura, M. Hanfland, and K. Syassen, Phys. Rev. Lett. **81**, 2711 (1998).

[7] M. Hanfland, U. Schwarz, K. Syassen, and K. Takemura, Phys. Rev. Lett. **82**, 1197 (1999).

[8] K. Takemura, O. Shimomura, and H. Fujihisa, Phys. Rev. Lett. **66**, 2014 (1991).

[9] K. Takemura, N.E. Christensen, D.L. Novikov, K. Syassen, U. Schwarz, and M. Hanfland, Phys. Rev. B **61**, 14399 (2000).

[10] M.I. Katsnelson, G.V. Sinko, N.A. Smirnov, A.V. Trefilov, and K. Yu. Khromov, Phys. Rev. B **61** 14420 (2000).

[11] D. Glötzel and A. K. McMahan, Phys. Rev. B**20**, 3210 (1979).

[12] N. E. Christensen, D. L. Novikov, and M. Methfessel, Solid State Commun. **110**, 615 (1999).

[13] N.E. Christensen, D.J. Boers. J.L. van Velsen, and D.L. Novikov, Phys. Rev. B **61**, R3764 (2000).

[14] N.E. Christensen, D.J. Boers. J.L. van Velsen, and D.L. Novikov, J. Phys.: Condens. Matter **12**, 3293 (2000).

[15] U. Schwarz, K. Syassen, A. Grzechnik, and M. Hanfland, Solid State Commun. **112**, 319 (1999).

[16] R. Ahuja, O. Eriksson, and B. Johansson, Phys. Rev. B **60**, 14475 (1999).

[17] K. Takemura, U. Schwarz, K. Syassen, N.E. Christensen, D.L. Novikov, and I. Loa, Phys. Rev. B **62**, R10603 (2000).

[18] K. Takemura, U. Schwarz, K. Syassen, M. Hanfland, N.E. Christensen, D.L. Novikov, and I. Loa, in Proceedings of the conference on *High Pressure in Semiconductor Physics 9* (HPSP9), Sapporo, Japan, September 2000, to appear in phys. stat. solidi.

[19] R. Sternheimer, Phys. Rev. **78**, 235 (1950).

[20] A. K. McMahan, Phys. Rev. B**29**, 5982 (1984).

[21] N. E. Christensen, Z. Pawlowska, and O. K. Andersen, unpublished. (1986).

[22] H.G. von Schnering pointed this out in a private communication.

[23] A.F. Wells, *Structural Inorganic Chemistry*, Oxford University Press, Oxford, UK, 1982.

[24] J.S. Kasper and S.M. Richards, Acta Crystallogr. **17**, 752 (1964).

[25] R.O. Piltz, J.R. Maclean, S.J. Clark, G.J. Ackland, P.D. Hatton, and J. Crain, Phys. Rev. B **52**, 4072 (1995).

[26] J. P. Perdew, K. Burke, and M. Ernzerhof, Phys. Rev. Lett., **77**, 3865 (1996).

[27] O.K. Andersen, Phys. Rev. B **12**, 3060 (1975).

[28] M. Methfessel, Phys. Rev. B **38**, 1537 (1988).

[29] D.J. Singh, *Planewaves, Pseudopotentials and the LAPW Method*, Kluwer Academic Publishers, Boston 1994.

[30] P. Blaha, K. Schwarz, P. Dufek and R. Augustyn, WIEN97, Technical University of Vienna 1997. (Improved and updated Unix version of the original copyrighted WIEN-code, which was published by P. Blaha, K. Schwarz, P. Sorantin and S.B. Trickey, Comput. Phys. Commun., **59**, 399 (1990).

[31] N.E. Christensen and D.L. Novikov, (to be published).

[32] See, for example, F. Herman and S. Skillman, *Atomic Structure Calculations*, Prentice-Hall, Inc., Englewood Cliffs, New Jersey (USA), 1963.

[33] N.E. Christensen and D.L. Novikov, Int. Journ. Quantum Chem. **77**, 880 (2000).